



# Time-resolved charge detection and back-action in quantum circuits

T. Ihn <sup>\*</sup>, S. Gustavsson, U. Gasser, R. Leturcq, I. Shorubalko, K. Ensslin

*Solid State Physics Laboratory, ETH Zurich, CH-8093 Zurich, Switzerland*

## ARTICLE INFO

Available online 3 December 2009

### Keywords:

Quantum point contacts  
Charge detection  
Quantum dots  
Back-action  
Quantum measurement

## ABSTRACT

This paper reviews investigations of back-action phenomena occurring in systems, where quantum dots are capacitively coupled to quantum point contact charge detectors. Two back-action mechanisms are discussed: first, back-action caused by shot-noise in the quantum point contact, and second, indirect back-action via ohmic heating of the crystal lattice. Experiments focusing on the first aspect consist of the measurement of shot noise at finite frequencies in the range between 0.01 and 0.7 THz. Experiments of the second kind result in the observation of finite current through a double quantum dot system at zero applied source–drain bias voltage. Such a current is possible in the presence of a phonon-system which is not in thermodynamic equilibrium with the electronic system. The double quantum dot acts as a thermoelectric engine extracting electric power from the temperature difference between the two thermal reservoirs.

© 2010 Elsevier B.V. All rights reserved.

## 1. Introduction

Measurements on quantum systems differ appreciably from measurements on classical systems. This has been recognized already by the founders of quantum mechanics [1–3]. Later, the topic has developed into a field of research of its own [4]. In recent years the topic has become of particular importance in the field of quantum information. While physical systems representing classical bits can be measured, or read-out, many times in succession without degrading the information content, the measurement of a quantum system representing a qubit usually changes the qubit state and thereby the associated information [5]. Commonly, this general phenomenon is called quantum back-action [4].

Electrons and their spins in semiconductor quantum dots can be utilized as particular realizations of quantum mechanical two-level systems, either in the form of spin-qubits [6] or charge qubits [7]. Controlled and coherent time evolution of these qubit implementations was demonstrated in a number of experiments [7,10,11]. Quantum point contacts were shown to be useful on-chip charge detectors [8,9] that allow one to read out the charge state of such qubits [12,13]. The use of these quantum point contact detectors triggered intense research in recent years where on-chip charge detection was utilized in a much broader context [14].

In this paper recent experiments will be discussed that aimed at an understanding of back-action phenomena related to the

measurement of the charge state of quantum dot systems. The paper is organized as follows: In Section 2 the charge detection technique will be briefly introduced. In Section 3 it will be shown how nonequilibrium shot noise present in a quantum point contact charge detector at finite source–drain bias voltage acts back on the quantum dot system. It turns out that the finite frequency shot noise spectrum can be investigated in detail. In Section 4 experiments are described in which the operation of the quantum point contact detector heats the host crystal. As a consequence, the phonon bath is no longer in equilibrium with the electronic system of the quantum dot circuit. This indirect back-action mechanism can drive currents through the quantum dot system even in the absence of an externally applied bias voltage.

## 2. Charge detection

We start the discussion by introducing the concept of charge detection with quantum point contact detectors. For this purpose we consider a setting as it is schematically depicted in Fig. 1. The first important part are two coupled quantum dots that can trap electronic charges. An additional charge can be trapped either in the upper or in the lower quantum dot. Quantum tunneling between the two dots provides the coupling between them rendering it a quantum mechanical two-level system, or a charge qubit. The second important part is the quantum point contact, a narrow constriction in a wire that supports a current, if a source–drain bias voltage is applied using an external voltage source. The magnitude of this current is determined by the width of the constriction. The two subsystems, i.e. the constriction and

<sup>\*</sup> Corresponding author. Tel.: +41 1 6332280; fax: +41 1 6331146.  
E-mail address: [ihn@phys.ethz.ch](mailto:ihn@phys.ethz.ch) (T. Ihn).

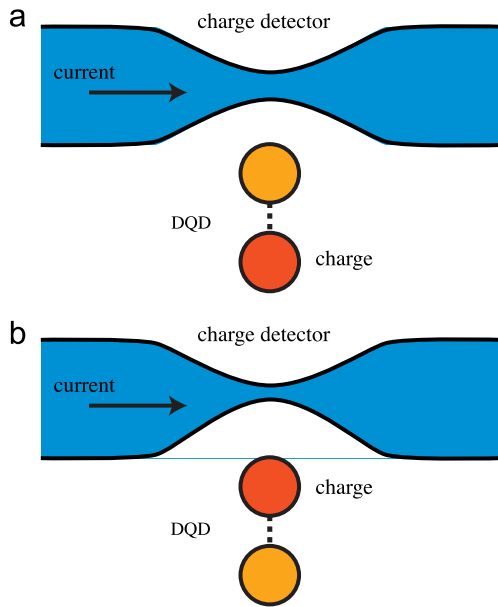


**Fig. 1.** Schematic diagram of a double quantum dot system (DQD) coupled capacitively to the narrow electronic channel of a quantum point contact (charge detector). (a) An additional charge occupies the lower quantum dot, the charge detector channel is more open and has a higher conductance. (b) The additional charge occupies the upper quantum dot, the charge detector channel is more closed and has a lower conductance.

the system of coupled quantum dots, are mutually coupled by the Coulomb interaction between their electrons. For example, if an additional electron is put into the lower quantum dot, the quantum point contact constriction is more open than if the electron is put into the upper quantum dot, as a result of the repulsive Coulomb potential of the added electron which reduces the width of the constriction. As a consequence, the current through (the conductance of) the quantum point contact is higher in the former case, as compared to the latter. We can state that the current through the quantum point contact allows us to detect the charge state of the double quantum dot system. This is the essence of the on-chip charge detection technique.

After the introduction of this technique [8], there has been a lot of interest in this quantum measurement system from the theoretical point of view. For example, it was investigated, how the measurement process with this charge detector results in decoherence of the dynamics in the coupled quantum dot system [15–20]. The relation between measurement and information was worked out for this system in detail [21], and it was shown that the quantum limit of detection can be reached, if the quantum point contact is adiabatic, and if the scattering phases fulfill a certain criterion. In general, this quantum limit of detection exists, because there is unavoidable back-action from the detector to the coupled quantum dot system. However, experimentally this quantum limit has not been demonstrated so far. Therefore, the understanding of back-action mechanisms is of great interest.

Before entering a more detailed discussion of back-action mechanisms we will briefly mention experimental work that has made use of the charge detection technique in various experimental systems. Charge detection has been demonstrated in lateral semiconductor nanostructures based on two-dimensional electron gases in Ga[Al]As heterostructures [8,9]. These first experiments were conducted with single quantum dots and at detector bandwidths which were low compared to the tunneling rates in the quantum dot systems, giving only information about time-averaged quantum dot charge. Later on, higher band with measurements on quantum dots with very small tunneling rates

allowed the detection of individual electrons hopping one by one into and out of the quantum dot system in real time [12,14,22]. The quantum point contact shows a characteristic random telegraphic current signal that witnesses the statistical tunneling of electrons from and into the quantum dot. The measurement bandwidth in these experiments was limited to about 40 kHz. A review of time-resolved charge detection experiments including the measurement of the full counting statistics of electron transport through quantum dots [24] can be found in Ref. [14]. Beyond the experimental work on time-resolved charge detection in single quantum dot systems, the technique has been extended to double quantum dots in the same material system [23,25], but also to InAs quantum dots [26] and quantum dots in graphene, where measurements without time resolution have been reported [27]. However, here we do not pursue the topic of electron counting further, but investigate the question, how the detector acts back on the measured system.

### 3. Back-action via shot noise

Conceptually, the investigation of back-action means to interchange the role of the measured system (in our case the quantum dots) and the detector (in our case the quantum point contact, cf. Fig. 1). A number of experiments in this direction have been reported in Refs. [9,28,29] where controlled decoherence as a result of a detection process was studied. We are interested in the influence of a quantum point contact charge detector on tailored single- and double quantum dot systems. Here we look at the direct action of the quantum point contact finite frequency shot noise on the dynamics of quantum dot systems.

We start by describing what shot noise is, and how it comes about. Finite frequency shot noise in quantum point contacts arises, if a finite source–drain bias voltage  $V_{SD}$  is applied. It is related to the statistical emission and absorption of energy quanta  $\hbar\omega$ . The power spectral density of the quantum point contact shot noise has, for example, been worked out in Ref. [30]. Here we are only interested in the emission side of the spectrum in the pinch-off regime, which is given by

$$S_I(\omega) = \frac{4e^2}{h} \mathcal{T}(1-\mathcal{T}) \frac{eV_{SD} - \hbar\omega}{1 - e^{-(eV_{SD} - \hbar\omega)/k_B T}}, \quad (1)$$

where  $\mathcal{T}$  is the transmission of the quantum point contact, and  $T$  is the electron temperature in the reservoirs. Fig. 2 shows a graphical representation of Eq. (1). At zero frequency (and zero temperature), the power spectral density takes the familiar value  $2|e|I(1-\mathcal{T})$  which has been experimentally investigated by a number of groups [31]. Here,  $I = 2e^2 \mathcal{T} V_{SD} / h$  is the current through the quantum point contact. The zero-frequency shot noise is maximum, if the transmission of the quantum point contact is  $\frac{1}{2}$ .

In the following we are interested in finite frequency shot noise. At finite frequency, the power spectral density decreases

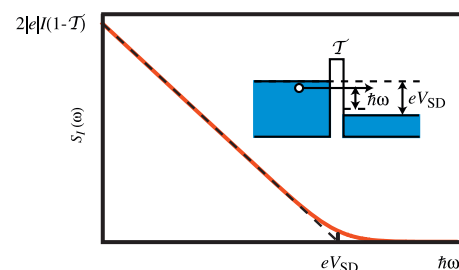


**Fig. 2.** Emission part of the shot noise power spectral density of a quantum point contact at zero temperature (dashed) and at finite temperature (solid). The inset shows a schematic quantum point contact potential under finite  $V_{SD}$  conditions.

linearly with  $\hbar\omega$ . At zero temperature, the maximum energy that can be emitted by the quantum point contact is given by the applied bias voltage  $|e|V_{SD}$  as evident from the inset of Fig. 2. On the other hand, according to Eq. (1) the power spectral density increases linearly with the applied bias voltage. The thermal denominator in Eq. (1) leads to the thermal smearing of  $S_I(\omega)$  around  $\hbar\omega = eV_{SD}$  seen in Fig. 2.

We will now look at two experiments that essentially confirm the form of the shot noise formula (1) in detail. The first experiment [26] relies on a quantum dot formed in an InAs quantum wire. Fig. 3 shows the sample and the external circuitry. A quantum wire has been deposited on top of a Ga[Al]As heterostructure hosting a shallow (34 nm) two-dimensional electron gas. In a single wet chemical etching step, two shallow trenches were etched into the substrate such that a quantum point contact was formed, and the wire was thinned down above the trenches such that a quantum dot was formed in the wire. In this system the quantum dot and the quantum point contact detector are very close to each other (about 80 nm) and perfectly aligned. As a consequence, the electrostatic coupling between the two systems is very strong. A suitable quantity characterizing the strength of the coupling is the change  $\Delta G$  of the detector conductance  $G$  when a single electron is added to the dot. In this device we found  $\Delta G/G$  values up to 50%, whereas in lateral devices usually only a few percent are achieved. Another special property of this arrangement is that phonons resulting from current-heating in the heterostructure quantum point contact cannot easily propagate into the InAs material. This setup is therefore optimized to maximize the quantum dot sensitivity to shot noise in the quantum point contact which is known as a primary source of charge detector back action.

The finite frequency shot noise is measured at a fixed frequency by using a ground-state–excited-state transition in the quantum dot. The energy difference between the two states is 2.5 meV corresponding to a frequency of 0.66 THz. The processes are schematically depicted in Fig. 4. The cycle starts, for example, with the ground state occupied with an excess electron. A virtual photon originating from the QPC shot noise kicks the system into the excited state with the rate  $\Gamma_{abs} \propto S_I(\omega)$ . From the excited state the electron will usually directly relax back into the ground state with a rate  $\Gamma_{rel}$  corresponding to something like 10 ns (not indicated in the figure). This relaxation time is believed to be by far the shortest timescale in the problem. As a result, only a small average population of the excited state will build up. The small probability to find the system in the excited state is given by  $p_e \approx \Gamma_{abs}/\Gamma_{rel}$ . This small population is probed by an even smaller tunneling coupling  $\Gamma_{es}$ , such that the tunneling out rate is  $\Gamma_{out} = p_e \Gamma_{es} \propto \Gamma_{abs} \propto S_I(\omega)$ . The tunneling-out rate is detected by a time-resolved measurement of the quantum point contact

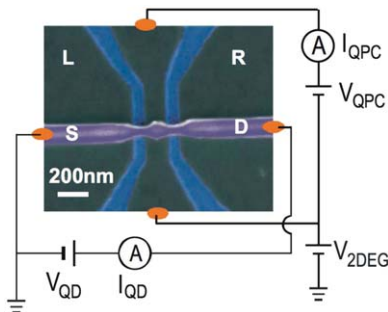


Fig. 3. Quantum dot in an InAs quantum wire on top of a Ga[Al]As heterostructure hosting a two-dimensional electron gas in which a quantum point contact has been formed by wet chemical etching.

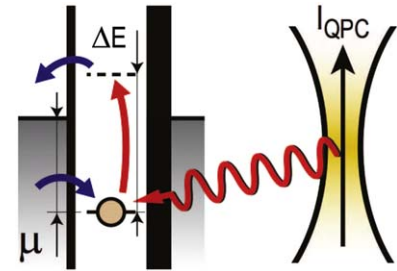


Fig. 4. Schematic energy diagram showing how the quantum dot can be excited by a photon originating from the quantum point contact.

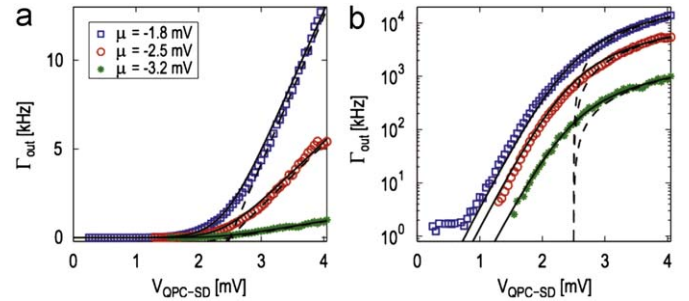


Fig. 5. Measured tunneling-out rate as a function of the quantum point contact bias voltage  $V_{SD}$  plotted on a linear scale (a) and a logarithmic scale (b). Solid lines represent fits to the shot noise formula, Eq. (1).

conductance itself. The cycle is closed by refilling an electron from below the Fermi energy into the quantum dot.

Fig. 5 shows the measured tunneling-out rate  $\Gamma_{out}$  as a function of the quantum point contact source–drain bias voltage  $V_{SD}$ . The measurement shows the linear increase of the tunneling-out rate predicted by the power spectral density  $S_I(\omega)$ . The onset of the linear increase is at  $V_{SD} = 2.5$  mV corresponding to the ground-state–excited-state transition energy. The logarithmic plot of  $\Gamma_{out}$  in Fig. 5(b) allows to identify the thermal denominator in Eq. (1). The three measurements shown in Fig. 5 have been performed for different values of the ground state energy measured relative to the electrochemical potential in the contact (denoted  $\mu$  in Fig. 4). If  $\mu$  approaches the quantum dot excitation energy, the measured tunneling out rate is suppressed, because the electron in the excited state finds an increasing number of occupied states in the contact.

Another aspect of the shot noise formula in Eq. (1) can be investigated, if the quantum point contact transmission is set to different values between zero and one. Care has to be taken that the quantum point contact still remains sensitive to changes of the quantum dot charge state (experimentally this excludes measurements in a regime where  $T$  is too close to one). It has been shown in Ref. [26] that the  $T(1-T)$ -dependence can indeed be reproduced with reasonable accuracy.

A shortcoming of the single quantum dot noise detection described above is the fact that the frequency dependence of the spectral density  $S_I(\omega)$  cannot be directly measured, because the ground-state to excited-state energy difference cannot be tuned. This problem can be overcome by coupling the quantum point contact to a double quantum dot system. This idea is related to the concept of using a double quantum dot as an energy tunable detector theoretically explored in Refs. [32,33]. Experiments along these lines have been performed in Ref. [25], where the structure was based on lateral patterning of a two-dimensional electron gas. The basic idea of this measurement is depicted in Fig. 6. The

double quantum dot system is tuned to a regime, where an electron can be excited from the ground state in the right dot to the excited state in the left dot. The detuning energy  $\Delta$  is the excitation energy of the system. It can be set to any value between the minimum given by the tunneling coupling between the dots and the maximum given by the smallest excitation energy within any of the two dots. In our experiment tuning was possible between 80 and 300  $\mu\text{eV}$  corresponding to photon frequencies between 20 and 80 GHz. Like in the previous experiment, the absorption rate of a photon from the quantum point contact shot noise  $S_I(\omega)$  is  $\Gamma_{\text{abs}}$ . Its value is small compared to the relaxation rate from the excited state into the ground state  $\Gamma_{\text{rel}}$  (not indicated in Fig. 6), such that a small excited state population  $p_e$  is built up, which can be probed with a small tunneling coupling  $\Gamma_{\text{es}}$  of the excited state to the contact, exactly like in the previous experiment.

The result of the corresponding measurement of the finite frequency shot noise as a function of  $\Delta$  is shown in Fig. 7. The decrease is, within measurement accuracy, linear with level

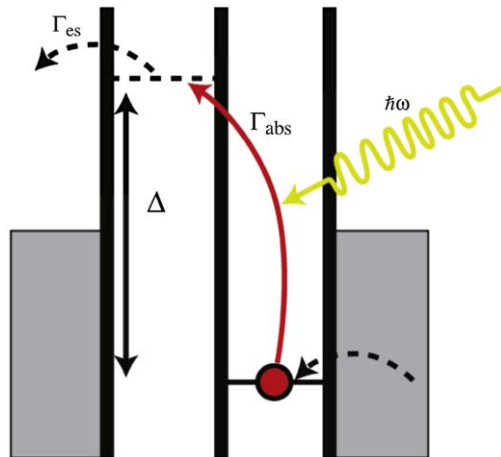


Fig. 6. Schematic energy diagram of a double quantum dot system used as an energy tunable detector for energy quanta. In the case of shot noise experiments the energy quanta are photons emitted from the quantum point contact.

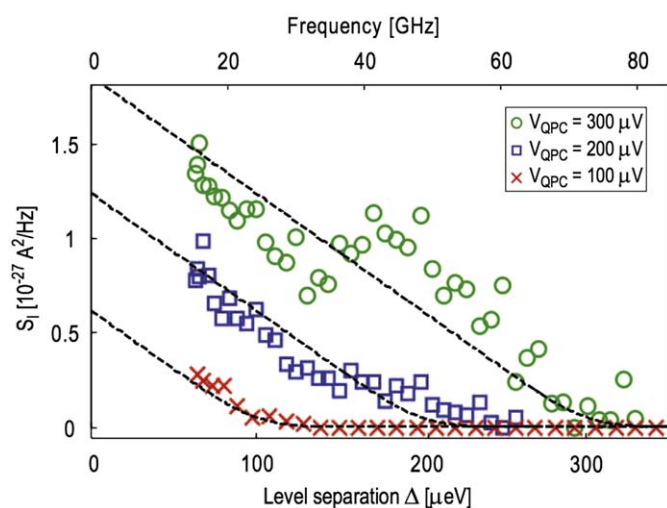


Fig. 7. Measured power spectral density of the finite frequency shot noise as a function of the excitation energy  $\Delta$ . Dashed lines represent fits to the shot noise formula, Eq. (1). The three curves were measured for three different source–drain bias voltages applied to the quantum point contact.

separation  $\Delta$ , i.e. with excitation energy  $\hbar\omega$ , in agreement with the prediction of Eq. (1). The dashed lines in the figure represent the expected outcome according to this formula. The three curves were measured for different source–drain voltages applied to the quantum point contact detector. Correspondingly, the finite frequency cut-off occurs at different energies corresponding to the values of these voltages.

Summarizing the experimental findings of this section, we can state that all details of the finite-frequency shot noise spectrum given by the power spectral density  $S_I(\omega)$  in Eq. (1) have been confirmed by the experiments described above. The results comprise the dependence on the quantum point contact source–drain bias voltage, the thermal smearing close to the cut-off frequency, the  $\mathcal{T}(1-\mathcal{T})$ -dependence on the quantum point contact transmission, and the frequency dependence.

#### 4. Indirect back-action via ohmic heating of the phonon bath

We now turn our attention to a different, indirect back-action mechanism [34]. The basic idea of this experiment can be well illustrated with Fig. 6. This figure does not contain any reference to a particular source of the energy quanta  $\hbar\omega$ . While in the previous experiments, we have considered photons originating from the quantum point contact, we will now consider phonons excited in the host crystal in which the coupled quantum dot system is realized. In such a scenario, Fig. 6 illustrates a transport cycle in which phonons excite the double quantum dot system in such a way that an electron jumps from the right to the left dot. Although it will relax back in most of the cases, in some instances it can be expected to leave the left dot towards the left contact. In this case, the transport cycle is completed, when an electron is refilled into the ground state by tunneling into the right dot from the right contact. This implies that a finite electrical current can be measured in the circuit of the double quantum dot in the absence of an applied source–drain bias voltage.

However, general thermodynamic considerations involving entropy and the second law of thermodynamics immediately suggest that we could not generate a current without an applied bias, if the phonon bath and the electronic system were in thermodynamic equilibrium, as this would constitute a perpetual mobile. As a consequence, the current can only be generated, if the phonon bath is at a higher temperature than the electronic system. The system then acts as a thermoelectric generator: energy in the form of heat flows from the phonon bath into the electronic system. However, during this process electrical work is done by lifting an electron up in energy. This work can be extracted in the form of a current that may be pushed through a load. The general thermodynamic principle of this kind of thermoelectric engine is illustrated in Fig. 8.

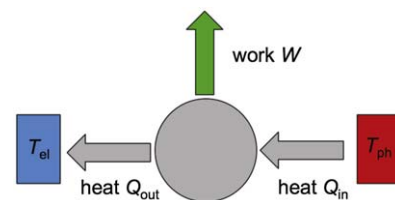


Fig. 8. Schematic illustration of the thermodynamic principle governing the generation of electrical power  $W$  in a thermoelectric engine, given that the electronic system (the electrons in the double quantum dot contacts) and the phonon system (lattice vibrations in the host crystal) are not in thermodynamic equilibrium, i.e.  $T_{\text{ph}} > T_{\text{el}}$ . Heat flows from warm to cold. As a side effect of the cleverly tuned double quantum dot levels with their built-in left–right asymmetry, a current is generated leading to the extraction of electrical power  $W$ . The first law of thermodynamics ensures that  $Q_{\text{in}} = Q_{\text{out}} + W$ .

How are these considerations related to the quantum point contact charge detector and its back-action? The answer is that the operation of the QPC unavoidably generates heat which will lead to an increased temperature of the phonon bath. From a quantum measurement perspective, this process can be regarded as the creation of entanglement between the phonon bath and the electronic circuit of the double quantum dot. Indeed, the measurements of Ref. [34] have been interpreted in this spirit using a dedicated microscopic theoretical description.

At this point we need to emphasize important differences between the double quantum dot experiments aiming at the detection of photons originating from shot noise in the quantum point contact detector, and the experiment to be described here. In the present experiment, the direct current through the double quantum dot was measured. In order to be able to do that, the coupling of the double quantum dot to source and drain contacts was orders of magnitude higher than in the experiments described above, where charge detection with time-resolution was used for detecting the occupation of the excited state. Two further differences ensued in the experiment described here that shot noise did not couple into the double quantum dot system: first, the quantum point contact was operated at the first conductance plateau where  $T \approx 1$  and therefore  $S_I(\omega) \approx 0$  (this precaution, however, turned out to be not crucial for the experimental results); second, a large area metallic top gate covering the double quantum dot and the quantum point contacts screened the Coulomb coupling between the two devices efficiently. Last but not least, the quantum point contact bias voltage was tuned to considerably higher values (up to 1 mV) than in the previous measurement on lateral coupled quantum dots.

Fig. 9 shows the current that has been measured in this experiment as a function of the detuning  $\Delta$  of the double quantum dot energy levels. No source–drain bias voltage was applied to the double quantum dot. Different curves in the figure correspond to different currents flowing through the quantum point contact. If the quantum point contact current is zero, no current can be driven through the double quantum dot, because the electronic system and the phonon bath are essentially in thermodynamic equilibrium. However, if a quantum point contact current of 100 nA is applied, a finite current of several hundred femtoampere through the double quantum dot is observed at nonzero detuning. The magnitude of the current flowing at positive detuning is much larger than that flowing at negative detuning. However, the sign of the current flow depends on the sign of the detuning. It is the detuning of the energy levels which creates the necessary asymmetry of the structure to give the current a preferential direction, similar to the case of a classical ratchet.

The observed data can be described in more detail if a microscopic model of the double quantum dot and its coupling to the phonon bath is invoked, as it was elaborated in Ref. [34]. In this model, the double quantum dot is described using a rate equation approach. It turns out that, within this model, the asymmetric shape of the observed current as a function of the detuning in Fig. 9 is due to the asymmetric tunneling coupling of the two dots to the respective contacts which can be confirmed independently by standard transport measurements. In the model, the coupling of electrons in the double quantum dot to acoustic phonons is taken into account in first order perturbation theory, allowing for deformation potential and piezoelectric coupling [34]. A number of form factors and energy-dependent coupling constants arising from the interaction matrix elements, as well as the energy-dependent phonon spectral density influence the detailed shape of the calculated current traces that are shown in Fig. 9 as solid lines.

In particular, the size of the two quantum dots makes phonon-coupling for large  $\Delta$  (large phonon wave vectors) inefficient and

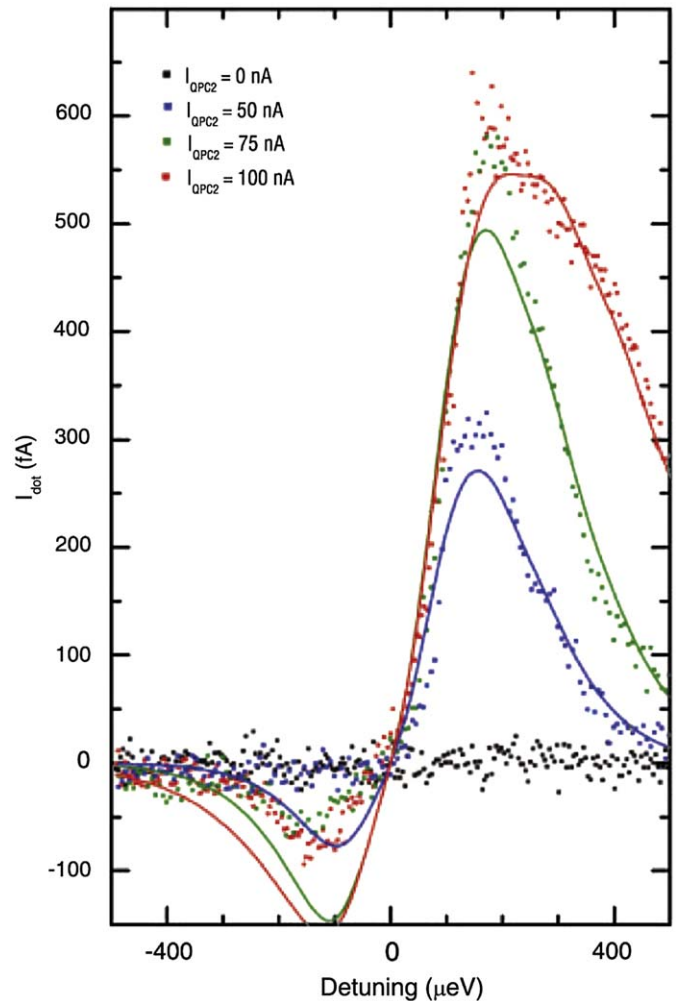


Fig. 9. Measurement of the current through the double quantum dot at zero applied source–drain bias voltage. Different measurement curves correspond to different currents applied to the quantum point contact. Solid lines are fits to a theoretical model.

contributes to the decrease of the measured current at large detuning. The wave function overlap between the relevant ground- and excited double quantum dot states (symmetric and antisymmetric state) decreases with increasing detuning, thereby adding another factor to the decrease of the measured current at large detuning. On the other hand, the increase of the measured current at low detuning is supported by a contribution to the form factor arising from the interdot separation  $d$  which suppresses transitions involving phonon wavelengths much larger than  $d$ . Additional contributions to the current increase at low detuning stem from the phonon density of states which increases with increasing energy, and the deformation potential and piezoelectric electron–phonon coupling constants. All these energy-dependent factors result in a response function of the double quantum dot that is large only in a small energy range with a maximum caused by the competition of factors increasing with energy and other factors decreasing in energy.

In order to keep the model as simple as possible, the phonon bath was assumed to be in thermal equilibrium at an effective temperature  $T_{ph}$ , whereas the electrons in the contacts of the quantum dot were assumed to be in thermal equilibrium at the temperature  $T_e$ . While  $T_e$  can be determined from the width of conductance resonances in the Coulomb blockade regime, the phonon temperature  $T_{ph}$  remains a fitting parameter for the

current calculated from the model that enters the spectral density of the phonon bath. In general, higher values of  $T_{\text{ph}}-T_{\text{e}}$  lead to larger phonon-induced current signals. Phonon temperatures extracted from the fits range from a few hundred millikelvin up to more than 1 K [34]. Similar experiments to those described here have been reported in Ref. [35].

## 5. Conclusion

In this paper we have reviewed experiments on direct and indirect back-action phenomena arising in setups where a quantum point contact charge detector is coupled capacitively to a quantum dot system. Direct back action was found in good agreement with the idea that nonequilibrium shot noise present in the detector couples back to the measured quantum dot system. The experiments allowed to identify all relevant characteristics of the predicted finite frequency shot noise spectrum in a frequency range between 0.01 and 0.7 THz. Indirect back-action could be successfully described using the model of a phonon bath heated by the operation of the quantum point contact detector. The basic physics behind this mechanism is in analogy with a thermoelectric engine converting heat into electric power utilizing the temperature difference between two equilibrium reservoirs. The experiments show that in systems, where the change in QPC current upon addition of a single electron to the double quantum dot is in the range of a few percent or above, and the QPC source–drain voltage is kept below about 1 mV, phonon related effects can be safely neglected in comparison to capacitive back-action effects. The findings described in this paper are therefore of great relevance for the operation of quantum point contact charge detectors as read-out devices for charge- or spin-qubits realized in semiconductor quantum dots.

## Acknowledgments

This research would not have been possible without world-class sample material from the groups of Werner Wegscheider, University of Regensburg and ETH Zurich, and Arthur Gossard, University of California, Santa Barbara.

## References

- [1] E. Schrödinger, *Naturwissenschaften* 23 (1935) 807; E. Schrödinger, *Naturwissenschaften* 823 (1935) 844.
- [2] A. Einstein, B. Podolsky, N. Rosen, *Phys. Rev.* 47 (1935) 777.
- [3] J. von Neumann, *Mathematische Grundlagen der Quantenmechanik*, Springer, Berlin, 1932 for an English translation see J. von Neumann, *Mathematical Foundations of Quantum Mechanics*, Princeton University Press, Princeton, NJ, 1955.
- [4] V.B. Braginsky, F.Y. Khalili, *Quantum Measurement*, Cambridge University Press, Cambridge, 1992.
- [5] M.A. Nielsen, I.L. Chuang, *Quantum Computation and Quantum Information*, Cambridge University Press, Cambridge, 2000.
- [6] D. Loss, D.P. DiVincenzo, *Phys. Rev. A* 57 (1998) 120; V. Cerletti, W.A. Coish, O. Gywat, D. Loss, *Nanotechnology* 16 (2005) R27.
- [7] T. Hayashi, T. Fujisawa, H.D. Cheong, Y.H. Jeong, Y. Hirayama, *Phys. Rev. Lett.* 91 (2003) 226804; T. Fujisawa, T. Hayashi, H.D. Cheong, Y.H. Jeong, Y. Hirayama, *Physica E* 21 (2004) 1046.
- [8] M. Field, C.G. Smith, M. Pepper, D.A. Ritchie, J.E.F. Frost, G.A.C. Jones, D.G. Hasko, *Phys. Rev. Lett.* 70 (1993) 1311.
- [9] E. Buks, R. Schuster, M. Heiblum, D. Mahalu, V. Umansky, *Nature* 391 (1998) 871.
- [10] F.H.L. Koppens, C. Buizert, K.J. Tielrooij, I.T. Vink, K.C. Nowack, T. Meunier, L.P. Kouwenhoven, L.M.K. Vandersypen, *Nature* 442 (2006) 766.
- [11] J.R. Petta, A.C. Johnson, J.M. Taylor, E.A. Laird, A. Yacoby, M.D. Lukin, C.M. Marcus, M.P. Hanson, A.C. Gossard, *Science* 309 (2005) 2180.
- [12] J.M. Elzerman, R. Hanson, J.S. Greidanus, L.H. Willems van Beveren, S. De Franceschi, L.M.K. Vandersypen, S. Tarucha, L.P. Kouwenhoven, *Phys. Rev. B* 67 (2003) 161308; J.M. Elzerman, R. Hanson, L.H. Willems van Beveren, B. Witkamp, L.M.K. Vandersypen, L.P. Kouwenhoven, *Nature* 430 (2004) 431.
- [13] J.R. Petta, A.C. Johnson, C.M. Marcus, M.P. Hanson, A.C. Gossard, *Phys. Rev. Lett.* 93 (2004) 186802.
- [14] T. Ihn, S. Gustavsson, U. Gasser, B. Küng, T. Müller, R. Schleser, M. Sigrist, I. Shorubalko, R. Leturcq, K. Ensslin, *Solid State Comm.* 149 (2009) 1419.
- [15] Y. Levinson, *Europhys. Lett.* 39 (1997) 299.
- [16] I.L. Aleiner, N.S. Wingreen, Y. Meir, *Phys. Rev. Lett.* 79 (1997) 3740.
- [17] S.A. Gurvitz, *Phys. Rev. B* 56 (1997) 15215.
- [18] M. Büttiker, A.M. Martin, *Phys. Rev. B* 61 (2000) 2737; M. Büttiker, S. Pilgram, *Surf. Sci.* 532–535 (2003) 617.
- [19] H.-S. Goan, G.J. Milburn, *Phys. Rev. B* 64 (2001) 235307.
- [20] A.N. Korotkov, *Phys. Rev. B* 63 (2001) 115403.
- [21] A.A. Clerk, S.M. Girvin, A.D. Stone, *Phys. Rev. B* 67 (2003) 165324.
- [22] R. Schleser, E. Ruh, T. Ihn, K. Ensslin, D.C. Driscoll, A.C. Gossard, *Appl. Phys. Lett.* 85 (2003) 2005.
- [23] T. Fujisawa, T. Hayashi, R. Tomita, Y. Hirayama, *Science* 312 (2006) 1634.
- [24] S. Gustavsson, R. Leturcq, B. Simovic, R. Schleser, T. Ihn, P. Studerus, K. Ensslin, D.C. Driscoll, A.C. Gossard, *Phys. Rev. Lett.* 96 (2006) 076605.
- [25] S. Gustavsson, M. Studer, R. Leturcq, T. Ihn, K. Ensslin, *Phys. Rev. Lett.* 99 (2007) 206804.
- [26] S. Gustavsson, I. Shorubalko, R. Leturcq, T. Ihn, K. Ensslin, S. Schön, *Phys. Rev. B* 78 (2008) 035324.
- [27] J. Güttinger, C. Stampfer, S. Hellmüller, F. Molitor, T. Ihn, K. Ensslin, *Appl. Phys. Lett.* 93 (2008) 212102.
- [28] D. Sprinzak, E. Buks, M. Heiblum, H. Shtrikman, *Phys. Rev. Lett.* 84 (2000) 5820.
- [29] I. Neder, M. Heiblum, D. Mahalu, V. Umansky, *Phys. Rev. Lett.* 98 (2007) 036803.
- [30] R. Aguado, L.P. Kouwenhoven, *Phys. Rev. Lett.* 84 (2000) 1986.
- [31] M. Reznikov, M. Heiblum, H. Shtrikman, D. Mahalu, *Phys. Rev. Lett.* 75 (1995) 3340; A. Kumar, L. Saminadayar, D.C. Glatli, Y. Jin, B. Etienne, *Phys. Rev. Lett.* 76 (1996) 2778; R. Liu, B. Odom, J. Kim, Y. Yamamoto, S. Tarucha, in: *Proceedings of the 23rd International Conference on the Physics of Semiconductors*, vol. 3, World Scientific, Singapore, 1996, p. 2399.
- [32] T. Gilad, S.A. Gurvitz, *Phys. Rev. Lett.* 97 (2006) 116806.
- [33] T. Geszti, J.Z. Bernad, *Phys. Rev. B* 73 (2006) 235343.
- [34] U. Gasser, S. Gustavsson, B. Küng, K. Ensslin, T. Ihn, D.C. Driscoll, A.C. Gossard, *Phys. Rev. B* 79 (2009) 035303.
- [35] V.S. Khrapai, S. Ludwig, J.P. Kotthaus, H.P. Tranitz, W. Wegscheider, *Phys. Rev. Lett.* 97 (2006) 176803.